RESEARCH ARTICLE
doi: 10.2306/scienceasia1513-1874.2026.006

ScienceAsia 51 (6): 2025: ID 2026006: **1–9**

Efficient purification of mouse Treg cells based on quantitative imaging full-spectrum flow cytometry

Yingying Huang[a], Xiaoyu Meng[b], Dan Yang[a], Yanwei Li[a], Jiajia Wang[a], Xin Shen[a], Shaoyun Chen[c,*]

[a] Core Facilities, School of Medicine, Zhejiang University, Hangzhou 310058 China
[b] School of Basic Medical Sciences, Zhejiang University, Hangzhou 310058 China
[c] School of Life Sciences, Zhejiang Chinese Medical University, Hangzhou 310053 China

*Corresponding author, e-mail: csy@zcmu.edu.cn

Received 2 Jan 2025, Accepted 18 Dec 2025
Available online 15 Jan 2026

ABSTRACT: An accurate and efficient method for the isolation and purification of Regulatory T (Treg) cells from primary mouse tissues was established based on the quantitative imaging full-spectrum flow cell sorter (BD FACSDiscover S8). The differences between this method and the traditional flow cell sorter (Aria II) were comprehensively evaluated. Additionally, the effects of different centrifugation conditions on the sorted cells were tested. The results demonstrated that the efficiency of S8, exceeding 94%, significantly outperforming Aria II. Under the conditions of EP (1.5 ml tubes centrifuged directly in the Eppendorf centrifuge) and 15 EP (1.5 ml centrifugal tube mounted on a 15 ml centrifugal tube and the samples centrifuged in a low-speed centrifuge), the yield after S8 sorting was not significantly different from that of Aria II, yet the viability of the former was superior. For samples sorted using either Aria II or S8, centrifugation under 15 EP conditions resulted in a lower cell apoptosis rate. The morphology of samples sorted by Aria II required microscope observation, which could not be used for objective quantitative analysis and had a low flux. In contrast, samples sorted by S8 could simultaneously captured cell morphology imaging while recording flow cytometry data, being fast and capable of analyzing the position and content of the target protein in the cell. This new method has high sorting efficiency, excellent viability, and a real-time image interaction function, which is applicable to the sorting of precious rare samples.

KEYWORDS: imaging flow cytometry, cell sorter, sorting efficiency, viability, yield of T cells

INTRODUCTION

Regulatory T cells (Treg cells), a CD4 subset discovered in 1995, account for approximately 10% of peripheral CD4+ T cells in normal rats and humans [1, 2]. Under steady-state conditions, they can suppress self-reactive immune responses, thus playing a crucial role in maintaining immune homeostasis. Additionally, Treg cells are also vital in maintaining self-tolerance and suppressing excessive immune responses in pathological processes such as infections [3–5]. Research on the function of Treg cells can effectively promote the development of Treg cell therapy, thereby providing robust support for alleviating the symptoms of related diseases or curing the disease. During development, Treg cells can be divided into thymus-derived regulatory T cells and peripherally derived Treg cells. Previous studies have confirmed that the expression of the transcription factor Foxp3 is a significant characteristic of Treg cells [6, 7]. The Scurfy phenotype, manifested as a severe systemic autoimmune inflammatory disease, is caused by the mutation of the Foxp3 gene [7–10]. People lacking Treg cells due to Foxp3 gene mutation exhibit IPEX (immune dysregulation, polyendocrinopathy, enteropathy, X-linked) syndrome [10–12]. Moreover, inducible deletion of the Foxp3 allele in mature Treg cells leads to the loss of their suppressive function and the acquisition of the ability to produce cytokines IL-2, IL-4, IL-17, and IFN-γ [13]. In summary, these data indicate that the continuous expression of Foxp3 is essential for maintaining the characteristics and suppressive function of Treg cells. Based on this, Treg cells isolated from tissues can be characterized by antibody labeling of Foxp3 and CD4/CD25, and the number and function of Foxp3+ Treg in organ tissues can be analyzed by flow cytometry [14]. However, since Foxp3 is located in the nucleus, fixation and permeabilization are required for staining during flow cytometry sample preparation. What's more unfortunate is that as fixed and permeabilized cells are relatively fragile, the cells sorted by traditional flow cell sorter are easily broken into fragments and thus cannot be applied to downstream research. Fortunately, in Foxp3$^{cre\text{-}YFP}$ transgenic mice, cells can initiate the transcription and translation of yellow-green fluorescent protein (YFP) while expressing Foxp3. Hence, all Foxp3+ cells can be labeled with YFP. By sorting out the live, unfixed, and unpermeabilized Treg subsets with YFP fluorescence, they can be used for further research, such as *in vitro* culture, single-cell sequencing, ATAC library construction, RNA-seq, Cut & Tag library construction, RT-PCR, Western blotting, and disease model establishment experiments.

Fluorescence-Activated Cell Sorting (FACS), which is based on flow cytometric analysis technology and uses flow cell sorters as experimental tools, can accurately separate populations or specific numbers of individual target cells or particles in mixed samples.

The separated target cells can be continuously cultured or used for other functional studies. Therefore, this technology is widely applied in disciplines such as immunology, pharmacology, oncology, cell biology, molecular biology, and plant breeding [15, 16]. However, traditional flow cell sorters lack image functions. As a result, the accuracy of the sorted samples is affected by subjective factors and false positive interferences from dead cells, fragments, or adhesion aggregates in the gating of flow charts and the sorting of target cells. In recent years, some new flow cytometers have come with image acquisition functions. For example, image flow cytometry was introduced into the analysis of crustacean blood cells [17]. Based on the differences in lateral scattering intensity and area that reflect the total amount of intracellular granular structure, the blood cells of Chinese mitten crabs can be clearly divided into four groups: large granular, medium granular, small granular, and non-granular blood cells. Freshwater phytoplankton in Beijing area was investigated through a flow imaging instrument (FowCAM) [18]. The results demonstrated that FowCAM reduced the time for sample pretreatment and increased the volume of measured samples compared to microscopic examination, presenting obvious advantages in cell counting. Ren et al [19] believed that image flow cytometers can identify more cell groups by using precise quantification standards compared to microscopic observation. They suggested that more refined classification results should be obtained by comprehensively using characteristic differences, and it is expected to be an important method for analyzing shellfish blood cells in the future. However, the image flow cytometers used in these works lack the function of sorting and recovering cells and cannot separate and purify target cells for further research.

The quantitative imaging full-spectrum flow sorter BD FACSDiscover S8 (hereinafter referred to as "S8") is the world's first and only flow cytometry instrument integrating the "image + full spectrum + cell sorting" three-in-one technology. BD's latest patented CellView technology truly realizes the "cross-border integration" of two classic technologies in the life science fields of flow cytometry and microscopy. It employs the new Spectral FX full-spectrum technology and is compatible with more than 130 dyes on the market. The sixth-generation holographic sorting technology not only enables seeing but also obtaining, realizing the true sense of "what you see is what you get". Once released, S8 won the cover of the top world journal Science [20] and the top medical journal NEJM [21], and was reported on the official website of the Ministry of Science and Technology of China for breaking through technical bottlenecks. Variations in sorting conditions will affect the viability, yield, and purity of target cells, with low-abundance cell populations, such as mouse Treg cells, being more susceptible to these effects [22, 26]. However, as of now, there is no report on using S8 to establish an accurate and efficient purification method for mouse Treg cells, despite the obvious benefits it would bring to the identification and characterization of Treg subsets and the study of their physiological state and unique biological functions in tissues.

Therefore, in this work, the latest model of flow cytometer S8 of BD Company in the United States was used as the debugging object. Taking mouse Treg cells as an example, by comparing the differences in sorting efficiency, purity, yield and viability between the quantitative imaging full-spectrum flow cytometer and the traditional flow cell sorter when sorting specific cell subsets, a new sorting and purification method for mouse Treg cells was established. This improves the efficiency of sorting experiments, thus providing technical references for related research and making the application of flow sorting technology and its cross-disciplinary integration with other technologies more extensive and in-depth.

MATERIALS AND METHODS

Equipment, reagents and materials

The quantitative imaging full-spectrum flow cytometer (BD FACSDiscover S8) and flow cytometer (BD Aria II) were purchased from BD Company, USA. The flow cytometer (CytoFlex S) was obtained from Beckman Coulter Company, USA. The phosphate PBS buffer was purchased from Medicago Company, Sweden. The Annexin V fluorescent double staining apoptosis kit (catalogue number ap105-100) was acquired from Lianke Biotechnology Co., Ltd. in Hangzhou, China. Foxp3$^{cre\text{-}YFP}$ transgenic mice, graciously provided by Professor Wang of Zhejiang University, were all approximately 6 to 8 weeks old and were reared in the SPF (Specific Pathogen Free) sterile environment of the Animal Experiment Center in School of Medicine at Zhejiang University. Sterile cell sieves, sterile flow tubes, and 15 ml centrifuge tubes were sourced from Corning Company, USA.

Preparation of lymphocyte samples

Foxp3$^{cre\text{-}YFP}$ transgenic mice aged 6 to 8 weeks were euthanized by spinal dislocation and then soaked in 75% alcohol. In a biosafety cabinet, the mouse lymph nodes were isolated and grounded to form a single-cell suspension. This suspension was then filtered into a 15 ml centrifuge tube using a 200-mesh nylon membrane. After that, it was centrifuged at 4 °C and 1,500 rpm for 5 min. The supernatant was discarded. Sorting buffer was added to resuspend the cells, and the cells were counted with a hemocytometer. The cell density of the single-cell suspension was adjusted to 1×10^8 cells/ml. According to experimental needs, an appropriate amount of cells was transferred to a sterile flow tube for standby.

Magnetic bead enrichment

The MojoSort™ Mouse CD4 T Cell Isolation Kit from Biolegend, USA, was employed in accordance with the instructions. Specifically, 10 µl of the antibody provided by the kit was added to every 100 µl of single-cell suspension, mixed well and incubated on ice for 15 min. Subsequently, the same volume of magnetic beads was added, mixed well and incubated on ice for another 15 min. Then, 2 ml of sorting buffer was added and thoroughly mixed. The sterile flow tubes were placed on a magnetic stand for 5 min. The supernatant was aspirated into a new 15 ml centrifuge tube. Finally, the cells were counted and used for subsequent experiments.

Sorting of mouse Treg cells by traditional flow cell sorter

The traditional flow cell sorter (BD Aria II, hereinafter referred to as "Aria II") was employed to sort mouse Treg cells with YFP fluorescence. Before sample sorting, all samples were filtered with a 40 µm sterile cell sieve and then loaded. A 1.5 ml centrifuge tube with 0.5 ml of PBS containing 10% (v/v) fetal bovine serum pre-added was used as the collection tube. For each sample, 100,000 events were collected. The sorting efficiency was recorded by the instrument software and then statistically analyzed. The identification of sorting purity was performed by rerun analysis using a flow cytometer immediately after sorting. Before the rerun analysis, the instrument needed to be fully cleaned.

Sorting of mouse Treg cells by quantitative imaging full-spectrum flow cell sorter

The instrument startup process was carried out in accordance with the instrument's user guide (Fig. 1). After the completion of quality control debugging, the prepared cell sample was placed into the sample inlet compartment. Fluorescence channel and image parameters were selected in turn, and then the pages "Adjust Gains" and "Set up single-Stain Controls" were clicked for debugging. Subsequently, image-related parameters such as Region of Analysis and Pixel Threshold on the 'View Data" page were adjusted, followed by clicking "Record" to record the flow cytometry and image data. After setting the sorting parameters on the "Set up Sort" page, the sorting was initiated. The collection tube preparation was the same as mentioned previously.

Centrifugation of sorted cells and exploration of different centrifugation conditions

The cells sorted by traditional flow cell sorter and quantitative imaging full-spectrum flow cell sorter were divided into two groups, respectively. In the first group, the sorted cells were centrifuged at 1,500 rpm for 15 min in an Eppendorf centrifuge (model: 5424R), which has an angle rotor (Fig. 2B). For the second group, the 1.5 ml centrifuge tube containing the sorted cells was placed on a 15 ml centrifuge tube (as shown in Fig. 2A), and centrifuged at 1500 rpm for 15 min in a low-speed centrifuge (model: TDL-50B), which has a horizontal rotor (Fig. 2C).

Cell counting and apoptosis detection

For the cells after centrifugation as described above, the supernatant was discarded. Then, 250 µl of 1× binding buffer (provided in the apoptosis kit) was added to resuspend the cells, followed by gently pipetting to ensure thorough mixing. For each sample, 50 µl was drawn and counted on the flow cytometer CytoFlex S, which had been volume-calibrated according to the instrument's own calibration program prior to the experiment. The remaining 200 µl of cells after counting were used for apoptosis detection. Apoptosis detection was conducted with reference to the instructions of the apoptosis detection kit (Annexin V-APC/7AAD apoptosis kit). For the above cells, 2 µl of Annexin V-APC and 4 µl of 7-AAD were added to each tube of sample. After thorough mixing, the samples were placed at room temperature away from light for 5 min and then subjected to flow cytometry analysis on CytoFlex S.

Microscopic morphological observation

The cells sorted by the Aria II instrument were thoroughly mixed. Subsequently, 200 µl of the cell suspension was drawn and dropped onto a clean glass slide and left to stand for 3 min. Afterward, the cell morphology was observed and photographed using an Olympus IX53 inverted fluorescence microscope, Olympus, Japan.

Statistical processing

All experimental data were statistically analyzed and graphed by GraphPad Prism 9.0 software, and the *t*-test was employed. Flow cytometry data were analyzed and plotted by FlowJo V10.7.1 software.

RESULTS

Comparison of instrument parameters and sorting efficiency related to sorting Treg cells

The parameters of the sorters are presented in Table 1. Both S8 and Aria II utilize an 85 µm nozzle and purity sort mode. The sample loading rate was adjusted so that the sample loading speeds of both instruments were maintained at approximately 10,000 evt/s with no significant difference. Under the condition of an 85 µm nozzle, the default sheath fluid pressure of S8 is 38 psi, while that of Aria II is 45 psi. The voltage of the sorting electrode plate and the threshold of sorting experiments employ the default parameters of the instrument. As can be seen from Fig. 3, the sorting efficiency of S8 was 94.67%, which was significantly

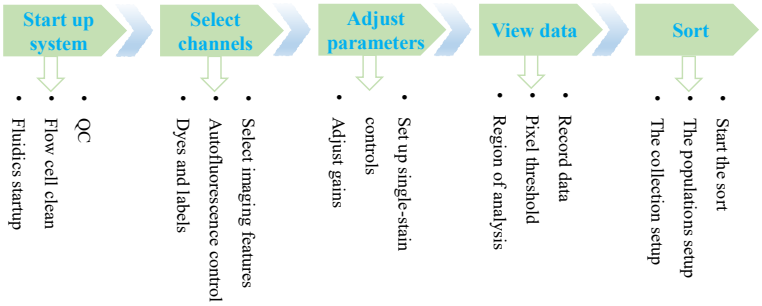

Fig. 1 Schematic diagram of sorting operation by quantitative imaging full-spectrum flow cell sorter.

Fig. 2 Different centrifugal methods of cells after sorting: (A) the 1.5 ml centrifugal tube is mounted on the 15 ml centrifugal tube; (B) centrifuge tube placement of Eppendorf centrifuge; (C) centrifuge tube placement of low-speed centrifuge.

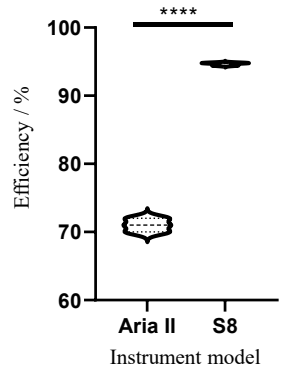

Fig. 3 Comparison of sorting efficiency of two sorting methods. Aria II: traditional flow cell sorter BD Aria II; S8: quantitative imaging full-spectrum flow cell sorter BD FACSDiscover S8. **** $p < 0.0001$, $n = 3$.

higher than the sorting efficiency of the traditional cell sorter Aria II.

Detection of Treg cell purity

As there are not many Treg cells in one mouse, which is insufficient for the quantity required for downstream experiments. Therefore, in this study, two mouse samples of the same genotype were sorted by loading samples, respectively. As shown in Fig. 4, for the sample sorted by Aria II, the percentage of Treg cells before purification was (5.1 ± 0.12)%; after purification, the purity of Treg cells was (98.6 ± 0.56)%. For the sample sorted by S8, the percentage of Treg cells before purification was (12.4 ± 0.31)%; after purification, the purity of Treg cells was (99.3 ± 0.70)%. After sorting, the purity measured by S8 was slightly higher than that measured by Aria II, but the difference between the two was not significant.

Influence of two sorting methods on cell recovery quantity

Respectively, 100,000 Treg cells were sorted by two sorting methods. Then, the yield of cells was compared after centrifugation. Since the 1.5 ml centrifuge tube used as the collection tube does not have a suitable horizontal rotor for centrifugation and can only utilize an angle rotor, while centrifugation with an angle rotor may impact the cell yield. Therefore, in this work, the influence of two different centrifugation methods (EP and 15 EP) on the cell yield was examined. As shown in Fig. 5, for the sample sorted by Aria II, the

Table 1 The parameters for sorting.

Instrument model	Nozzle size (μm)	Sheath pressure (psi)	Loading speed (evt/s)
BD FACSDiscover S8	85	38	10909 ± 60.38
BD Aria II	85	45	10759 ± 154.11

evt/s, events per seconds.

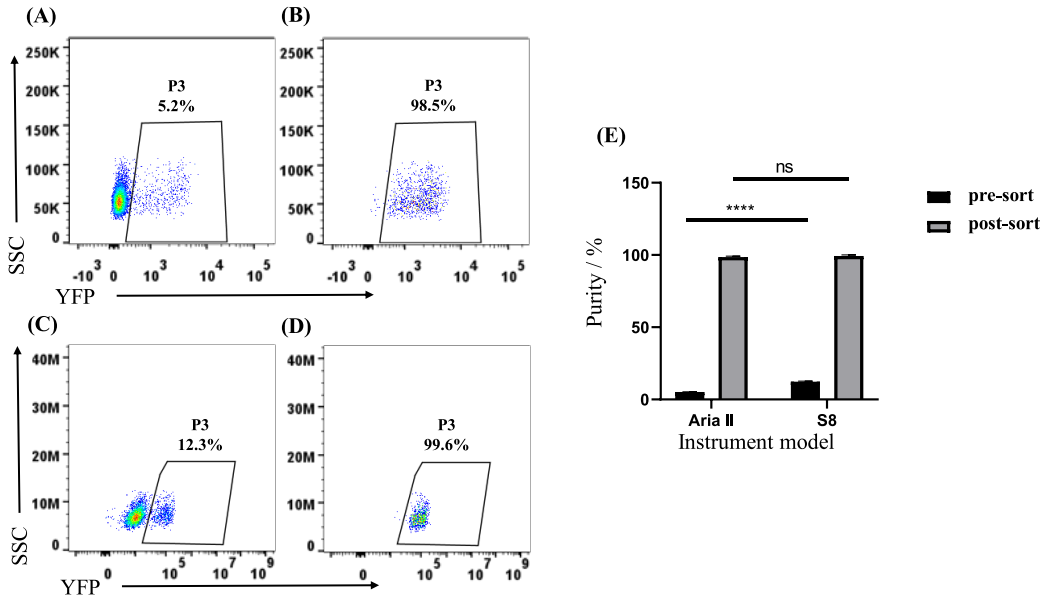

Fig. 4 Detection of the purity of Treg cells. Proportion of Treg cells, (A) before and (B) after sorted by traditional flow cell sorter Aria II; Proportion of Treg cells, (C) before and (D) after sorted by quantitative imaging full-spectrum flow cell sorter BD FACSDiscover S8; (E) comparison of purity of Treg cells post-sort by different instruments. ns: not significant; **** $p < 0.0001$, $n = 3$; YFP: yellow-green fluorescent protein; SSC: side scatter.

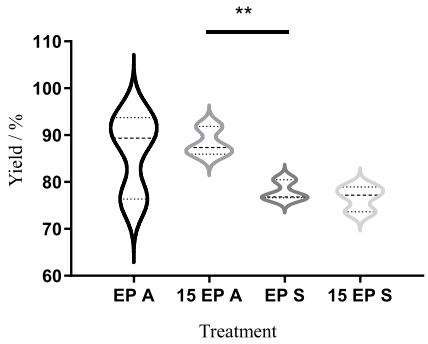

Fig. 5 Comparison of cell yield after sorting by different instruments. EP A: 1.5 ml tubes were centrifuged directly in the Eppendorf centrifuge, samples were sorted by Aria II; 15 EP A: the 1.5 ml centrifugal tube was mounted on the 15 ml centrifugal tube, then the samples which were sorted by Aria II were centrifuged in a low-speed centrifuge; EP S: same as EP A but the samples were sorted by S8; 15 EP S: same as 15 EP A but the samples sorted by S8 were centrifuged in a low-speed centrifuge. ** $p < 0.01$, $n = 3$.

yield after centrifugation in EP A was 86.47%, and the yield after centrifugation in 15 EP A was 88.38%. The difference between the two was not significant. For the sample sorted by S8, the difference in yield after centrifugation in EP A and yield after centrifugation in 15 EP A was also not significant. Under the same centrifugation conditions, there was no significance in the sample yield after sorting by Aria II and S8.

Comparison of cell viability after sorting

The sorted Treg cells were subjected to apoptosis experiments respectively. A higher apoptosis rate indicates lower viability of the sorted cells. In the EP A treatment, by directly centrifuging the 1.5 ml centrifuge tube in an Eppendorf centrifuge, the apoptosis rate of the sample sorted by Aria II was 26.19%, which was significantly higher than the apoptosis rate of the sample sorted by S8 ($p < 0.05$). By placing the 1.5 ml centrifuge tube on a 15 ml centrifuge tube and centrifuging in a low-speed centrifuge (hereinafter referred to as "15 EP"), the apoptosis rate of the sample sorted by Aria II was 8.51%, which was not significantly different from the apoptosis rate of the sample sorted by S8. However, the mean value of the former was still slightly higher than that of the latter (Fig. 6). This indicates that the sample cells sorted by S8 had better viability. Additionally, as shown in Fig. 6E, regardless of whether the samples were sorted by Aria II or S8, centrifugation under the condition of 15 EP resulted in a lower apoptosis rate.

Morphological observation of Treg cells

As depicted in Fig. 7, high-definition imaging of cells had been accomplished by S8. When the picture data was set to be from all cells (Fig. 7A), the picture wall displayed the morphology of all cells, including single cells and two or more adhered cells. Most cells lacked fluorescent signals, indicating that the proportion of Treg cells in mouse primary tissues was relatively low.

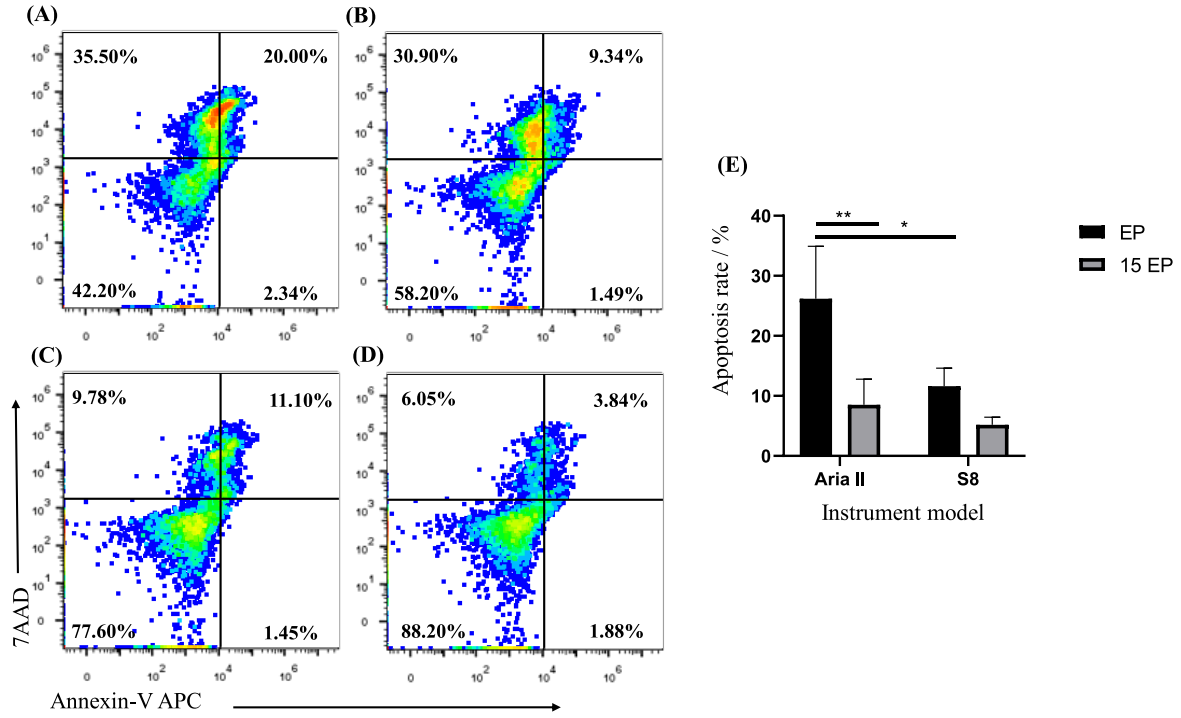

Fig. 6 Comparison of cell viability after sorting by different instruments. (A) EP A; (B) 15 EP A; (C) EP S; (D) 15 EP S; (E) comparison of viability of Treg cells after sorted by different instruments. Treatment codes are the same as those mentioned in legend of Fig. 5. * $p < 0.05$, ** $p < 0.01$, $n = 3$.

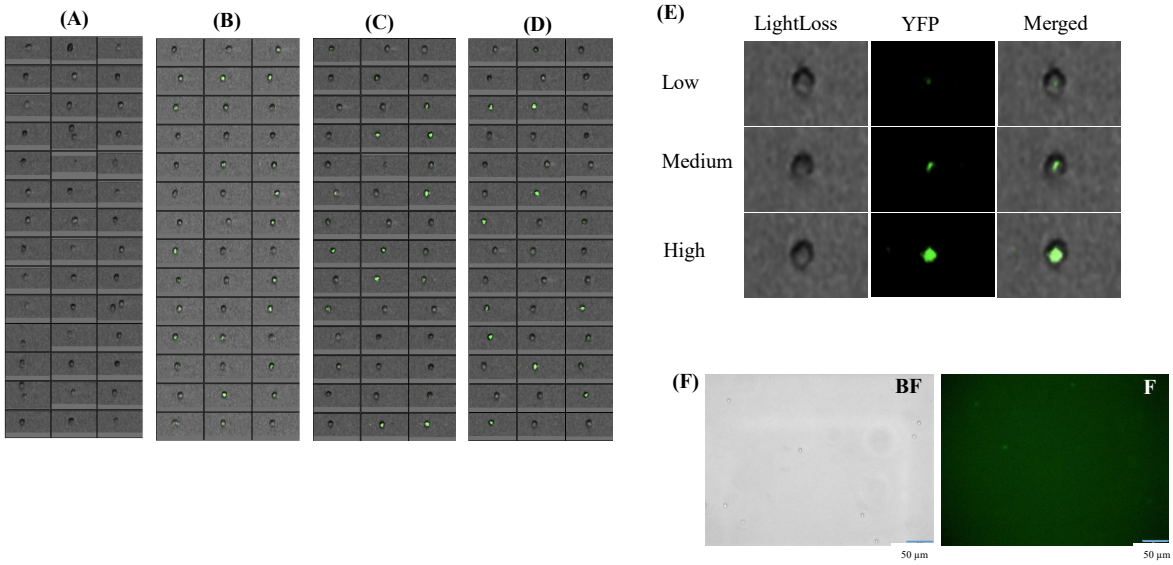

Fig. 7 Morphological observation of cells after sorting by different instruments. (A) and (B) picture wall of cells by S8 before sorting, cells from all events (A) and cells from the gate of YFP positive population (B); (C) and (D) picture wall of cells by S8 after sorting, cells from all events (C) and cells from the gate of YFP positive population (D); (E) morphological observation of Treg cells before sorting by S8; (F) the morphology of the Treg cells after sorting by Aria II were observed using an inverted fluorescence microscope; BF: bright field; F: fluorescence.

When the picture data was set to be from the YFP positive cell gate (this gating is from the removal of adhered cells, and the result is not shown), as shown in Fig. 7B, the picture wall clearly exhibited the morphology of all Treg cells. These are all round, uniform, and in good condition cells with different degrees of fluorescent signals (Fig. 7E), which is in accordance with the flow cytometry results. As can be seen from Fig. 7C and Fig. 7D, after sorting by S8, the morphology of Treg cells did not change significantly compared to before sorting.

The traditional flow cell sorter Aria II lacks an image function. Therefore, in this paper, Treg cells sorted by Aria II were placed under an inverted fluorescence microscope for observation. As shown in Fig. 7F, under bright field conditions, cells were in a uniform and round state, which is consistent with the imaging result of S8. However, in fluorescence mode, in some fields of view, cells could not be seen. In some fields of view, a few cells with green fluorescence could be occasionally seen. The signal was very weak and basically the same as the background.

Comprehensive comparison between quantitative imaging full-spectrum flow cell sorting and traditional flow cell sorting

As shown in Table S1, for sorting 100,000 Treg cells, the sorting time of S8 was 7 min, which was shorter than that of Aria II, under the same proportional gating (5.0% of Treg cells are circled) and the same sorting conditions. Although the startup time of the quantitative imaging full-spectrum flow sorter S8 is slightly longer than that of the traditional flow cell sorter Aria II. The position of the collection tube holder of S8 does not require manual calibration, which is relatively time-saving, labor-saving and objective. Regarding imaging, the samples sorted by Aria II need to be observed under a microscope for morphology. Aria II cannot perform objective quantitative analysis and has a low throughput. In contrast, the samples sorted by S8 can complete the imaging of cell morphology simultaneously when rerunning the purity. This is fast and can analyze the position and expression level of YFP in the cell (Fig. 7E). Moreover, the sample used for S8 sorting has no special requirements in sample preparation as in traditional flow cell sorting.

DISCUSSION

At present, various cell purification technologies exist, including density gradient centrifugation, immunomagnetic bead method, gravity sedimentation, and flow cell sorting method, among others. Flow cell sorting is widely employed in diverse downstream studies as it can separate heterogeneous cells into different subsets [22]. Traditional flow cytometers can achieve high-throughput acquisition of cell phenotype and protein quantification information but cannot directly analyze protein expression patterns and cell functions. Fluorescence microscopes can directly obtain cell morphological information yet are unable to perform objective quantitative analysis and have a low throughput. Imaging flow cytometry represents the combination of the depth and breadth of cell research. It integrates the statistical power of flow cytometry in cell phenotype analysis, the high speed, and high sensitivity of cell analysis, and the insight of fluorescence microscopy technology in the detailed analysis of cell morphology [23]. Therefore, based on BD FACSDiscover S8, this study established a new method of quantitative imaging full-spectrum flow purification for mouse Treg cells. By measuring indicators such as sorting efficiency, purity, yield, viability, experiment time consumption, and cell morphology of sorted cells, the differences between S8 and traditional flow sorting method were comprehensively compared.

For purification experiments conducted with flow cytometers, sorting purity, yield and activity are the main indicators for evaluating sorted cells. Additionally, sorting efficiency is a very important yet often overlooked parameter. As can be seen from Fig. 4 and Fig. 5, although there was no significant difference in the purity and yield of cells sorted by S8 and the traditional flow cell sorter, the sorting efficiency of S8 was greater than 94%, which was significantly higher than that of the traditional sorter Aria II (Fig. 3). This indicates that S8 could lead to more target cells per unit time and reduced the loss of target cells, making it more conducive to the sorting of precious and rare cells. This study also explored the impacts of two sorting methods on cell viability. The results demonstrated that the cell viability after sorting by S8 was higher than that of the sample sorted by Aria II (Fig. 6E). During apoptosis detection of the latter, more necrotic cells appeared, while there were fewer necrotic cells in the former (Fig. 6A–D). This might be due to the fact that the sample used in this study was a manually dissociated sample of mouse primary tissue and had undergone the step of immunomagnetic bead sorting and enrichment. The processing time was slightly longer, which affected the sample activity and can be improved in subsequent studies. However, it can be seen that when sorting and purifying cells in a not-so-good state, the activity of quantitative imaging full-spectrum flow sorting was superior to that of traditional flow sorting. In addition, under the same sorting parameters, the time for S8 to obtain an equal amount of target cells was less than the sorting time of Aria II (Table S1), and for the same nozzle, the default sheath fluid pressure of S8 was lower than that of Aria II (Table 1). All these factors might all contribute to make it easier for S8 to obtain highly active cells.

After flow cell sorting, the cell surface carries a certain charge. The same kind of charge repels each other, making centrifugation difficult. Previous studies [16] by our research group indicated that the

optimal centrifugation time for mouse primary cells after sorting was 15 min. Hence, in this study, the cells sorted by the two sorting methods were centrifuged for 15 min. Since functional experiments such as single-cell sequencing require a small amount of sample and a 1.5 ml centrifuge tube is needed as the sorting collection tube. However, this centrifuge tube does not have a suitable horizontal rotor for centrifugation and can only use an angle rotor. Centrifugation with an angle rotor cannot directly centrifuge all cells to the bottom of the tube. Whether this will affect cell yield and viability has not been reported previously. The innovative work of this paper is that for the first time, a 1.5 ml centrifuge tube containing sorted cells was placed on a 15 ml centrifuge tube and centrifuged on a horizontal rotor of a low-speed centrifuge (15 EP). The results show that compared with centrifugation with an angle rotor, there was no significant difference in the yield (Fig. 5). But for samples sorted by either Aria II or S8, centrifuging the cells under the condition of 15 EP resulted in better cell viability (Fig. 6E). Therefore, when a 1.5 ml centrifuge tube is used as the collection tube in a flow cell sorting experiment, centrifugation in the 15 EP way is recommended.

Microscopic observation has highly subjective when distinguishing cell types based on morphological characteristic similarities and differences. In contrast, flow measurement takes a single cell as the object and employs a precise detection module to conduct high-throughput analysis of the physical characteristic parameters of cells, yielding relatively objective results [24]. As can be seen from Fig. 7, Treg cells sorted by a traditional flow cell sorter were placed under an inverted fluorescence microscope for observation. In a single field of view, fewer cells were visible, and the expression level of YFP in Treg cells could not be distinguished. However, S8 could quickly complete the acquisition of image signals while recording flow cytometry data. The presented cell images are clear, the data is abundant, and it can distinguish the position and expression level of YFP in the cell (Fig. 7E). This enables us to objectively and accurately circle the flow cytometry gate and observe in a timely whether there is any change in the morphology of the sample before or after sorting. That is, a sample can give multi-dimensional experimental data, and the image and flow cytometry data interact in real time for intuitive confirmation. Sorting by gating through image parameters can further explore the spatial position and morphological information of the sample [25], which is beneficial for the development of downstream research, such as spatial omics, proteomics, and transcriptomics research.

In short, the new method of purification of mouse Treg cells by quantitative imaging full-spectrum flow cell sorter established in this paper had high sorting efficiency, short time consumption, high purity and yield of obtained cells, good viability, and the cell morphology in real time before and after sorting could be observed. It is suitable for the sorting of precious and rare samples or samples with high cell requirements for subsequent functional experiments and has important research significance and promotion and application value.

Appendix A. Supplementary data

Supplementary data associated with this article can be found at https://dx.doi.org/10.2306/scienceasia1513-1874.2026.006.

Acknowledgements: This work was supported by the Experimental Technology Research Project of Zhejiang University (Grant No. SYBJS202209) and Zhejiang Provincial Education Department Fund (Grant No. Y202454725).

REFERENCES

1. Sakaguchi S, Sakaguchi N, Asano M, Itoh M, Toda M (1995) Immunologic self-tolerance maintained by activated T cells expressing IL-2 receptor alpha-chains (CD25). Breakdown of a single mechanism of self-tolerance causes various autoimmune diseases. *J Immunol* **155**, 1151–1164.
2. Kitagawa Y, Wing JB, Sakaguchi S (2015) Transcriptional and epigenetic control of regulatory T cell development. *Prog Mol Biol Transl Sci* **136**, 1–33.
3. Sakaguchi S, Yamaguchi T, Nomura T, Ono M (2008) Regulatory T cells and immune tolerance. *Cell* **133**, 775–787.
4. Josefowicz SZ, Lu LF, Rudensky AY (2012) Regulatory T cells: Mechanisms of differentiation and function. *Annu Rev Immunol* **30**, 531–564.
5. Singer BD, King LS, D'Alessio FR (2014) Regulatory T cells as immunotherapy. *Front Immunol* **5**, 1–10.
6. Hori S, Nomura T, Sakaguchi S (2003) Control of regulatory T cell development by the transcription factor Foxp3. *Science* **299**, 1057–1061.
7. Fontenot JD, Gavin MA, Rudensky AY (2003) Foxp3 programs the development and function of CD4(+) CD25(+) regulatory T cells. *Nat Immunol* **4**, 330–336.
8. Brunkow ME, Jeffery EW, Hjerrild KA, Paeper B, Clark LB, Yasayko SA, Wilkinson JE, Galas D, et al (2001) Disruption of a new forkhead/winged-helix protein, scurfin, results in the fatal lymphoproliferative disorder of the scurfy mouse. *Nat Genet* **27**, 68–73.
9. Wildin RS, Ramsdell F, Peake J, Faravelli F, Casanova JL, Buist N, Levy-Lahad E, Mazzella M, et al (2001) X-linked neonatal diabetes mellitus, enteropathy and endocrinopathy syndrome is the human equivalent of mouse scurfy. *Nat Genet* **27**, 18–20.
10. Van Gool F, Nguyen MLT, Mumbach MR, Satpathy AT, Rosenthal WL, Giacometti S, Le DT, Liu W, et al (2019) A mutation in the transcription factor Foxp3 drives T helper 2 effector function in regulatory T cells. *Immunity* **50**, 362–377.
11. Bennett CL, Christie J, Ramsdell F, Brunkow ME, Ferguson PJ, Whitesell L, Kelly TE, Saulsbury FT, et al (2001) The immune dysregulation, polyendocrinopathy, enteropathy, X-linked syndrome (IPEX) is caused by mutations of FOXP3. *Nat Genet* **27**, 20–21.
12. Gambineri E, Torgerson TR, Ochs HD (2003) Immune dysregulation, polyendocrinopathy, enteropathy, and X-

linked inheritance (IPEX), a syndrome of systemic autoimmunity caused by mutations of FOXP3, a critical regulator of T-cell homeostasis. *Curr Opin Rheumatol* **15**, 430–435.
13. Williams LM, Rudensky AY (2007) Maintenance of the Foxp3-dependent developmental program in mature regulatory T cells requires continued expression of Foxp3. *Nat Immunol* **8**, 277–284.
14. Jiang X, Liu XN, Li B (2023) Flow cytometric analysis of regulatory T Cells from various mouse tissues. *Chin J Cell Biol* **45**, 902–910.
15. Wan YJ, Wang R, Zhang S, Zhou Y, Long JF (2024) Creative adjustment of the flow cell sorter and the application in the purification of naive T cells. *Exp Sci Technol* **22**, 8–13.
16. Huang YY, Xing YT, Meng XY, Sang WH, Li YW, Song XH, Guo C, Wang JJ (2021) Study on the influence of centrifugal parameters on the samples sorted by flow cell sorting. *Chin J Cell Biol* **43**, 2001–2008.
17. Hu JL, Ren XC, Liu YC, Sun JS, Geng XY, Zhang YC (2019) Application of imaging flow cytometry in studies of the classification and phagocytic function of *Eriocheir sinensis* blood cell. *J Fish China* **43**, 563–572.
18. Wang SS, Wan J, Zhao GP, Dong XW (2022) Investigation and research on freshwater phytoplankton in Beijing area by flow cytometer and microscope (FlowCAM) and microscopic. *Ecol Evol* **4**, 70–77.
19. Ren XC, Li R, Zhang N, Liu YC, Sun JS, Zhang YC (2020) Hemocytes classification of *Meretrix meretrix* and *Ruditapes philippinarum* by imaging flow cytometer. *J Anhui Agric Sci* **48**, 98–101.
20. Schraivogel D, Kuhn TM, Rauscher B, Rodríguez-Martínez M, Paulsen M, Owsley K, Middlebrook A, Tischer C, et al (2022) High-speed fluorescence image-enabled cell sorting. *Science* **375**, 315–320.
21. Filby A, Carpenter AE (2022) A new image for cell sorting. *N Engl J Med* **386**, 1755–1758.
22. Song X, Wang J, Li Y, Xing Y, Guo C, Huang Y, Xu L, Hu H, et al (2021) Improved strategy for jet-in-air cell sorting with high purity, yield, viability, and genome stability. *FEBS Open Bio* **11**, 2453–2467.
23. Konecny AJ, Mage PL, Tyznik AJ, Prlic M, Mair F (2024) 50-color phenotyping of the human immune system with in-depth assessment of T cells and dendritic cells. *Cytom Part A* **105**, 430–436.
24. Li R, Ren XC, Zhang N, Wang Y, Liu Y C, Zhang YC, Geng XY, Sun JS (2022) Imaging flow cytometry measurement and pathogens infection analysis of *Litopenaeus vannamei* hemocytes. *J Fish China* **46**, 1094–1103.
25. Sun J, Zhang Y, Zhang Q, Hu L, Zhao L, Wang H, Yuan Y, Niu H, et al (2024) Metabolic regulator LKB1 controls adipose tissue ILC2 PD-1 expression and mitochondrial homeostasis to prevent insulin resistance. *Immunity* **57**, 1289–1305.
26. Herppich S, Toker A, Pietzsch B, Kitagawa Y, Ohkura N, Miyao T, Floess S, Hori S, et al (2019) Dynamic imprinting of the Treg cell-specific epigenetic signature in developing thymic regulatory T cells. *Front Immunol* **10**, 2382.

Appendix A. Supplementary data

Table S1 Comparison of the two sorting methods.

Item	Traditional flow cell sorter Aria II	Quantitative imaging full-spectrum flow cell sorter S8
Boot time	45 min	60 min
Time-consuming	10 min	7 min
Collection device check	Manual	Automatic
Imaging speed	Slow, imaging with a microscope after sorting and the number of cells imaged per unit time is small.	Quick, the instrument itself can image the sample, >10,000 cells/s.
Imaging effect of primary Treg cells	Fluorescence microscope imaging is not clear, cannot distinguish the level of expression.	Clear, Treg cells expressing YFP protein signal can be clearly impictured, and the position and content of YFP expression in cells can be distinguished.
Special sample preparation requirements	None	None